2018

Structure of the Ambrosia Beetle (Coleoptera: Curculionidae) Mycangia Revealed Through Micro-Computed Tomography

You Li

Yongying Ruan

Matthew T. Kasson

Edward L. Stanley

Conrad P.D.T Gillett

See next page for additional authors

Authors

You Li, Yongying Ruan, Matthew T. Kasson, Edward L. Stanley, Conrad P.D.T Gillett, Andrew J. Johnson, Mengna Zhang, and Jiri Hulcr

Journal of Insect Science, (2018) 18(5): 13; 1–8
doi: 10.1093/jisesa/iey096
Research

Structure of the Ambrosia Beetle (Coleoptera: Curculionidae) Mycangia Revealed Through Micro-Computed Tomography

You Li,[1,†] Yongying Ruan,[2,†] Matthew T. Kasson,[3] Edward L. Stanley,[4] Conrad P. D. T. Gillett,[1] Andrew J. Johnson,[1] Mengna Zhang,[2] and Jiri Hulcr[1,5]

[1]School of Forest Resources and Conservation, University of Florida, Gainesville, FL, [2]School of Applied Chemistry and Biological Technology, Postdoctoral Innovation Practice Base, Shenzhen Polytechnic, Shenzhen, Guangdong, China, [3]Division of Plant and Soil Sciences, West Virginia University, Morgantown, WV, [4]Florida Museum of Natural History Department, University of Florida, Gainesville, FL, and [5]Corresponding author, e-mail: hulcr@ufl.edu

[†]You Li and Yongying Ruan are co-first authors.

Subject Editor: Phyllis Weintraub

Received 8 July 2018; Editorial decision 10 September 2018

Abstract

Ambrosia beetles (Coleoptera: Curculionidae: Scolytinae and Platypodinae) rely on a symbiosis with fungi for their nutrition. Symbiotic fungi are preserved and transported in specialized storage structures called mycangia. Although pivotal in the symbiosis, mycangia have been notoriously difficult to study, given their minute size and membranous structure. We compared the application of novel visualization methods for the study of mycangia, namely micro-computed tomography (micro-CT) and laser ablation tomography (LATscan) with traditional paraffin sectioning. Micro-CT scanning has shown the greatest promise in new organ discovery, while sectioning remains the only method with sufficient resolution for cellular visualization. All three common types of mycangia (oral, mesonotal, and pronotal) were successfully visualized and presented for different species of ambrosia beetles: *Ambrosiodmus minor* (Stebbing) 1909, *Euplatypus compositus* (Say) 1823, *Premnobius cavipennis* Eichhoff 1878, *Scolytoplatypus raja* Blandford 1893, *Xylosandrus crassiusculus* (Motschulsky) 1866 and *X. amputatus* (Blandford) 1894. A reconstruction of the mycangium and the surrounding musculature in *X. amputatus* is also presented. The advantages of micro-CT compared to the previously commonly used microtome sectioning include the easy visualization and recording of three-dimensional structures, their position in reference to other internal structures, the ability to distinguish natural aberrations from technical artifacts, and the unprecedented visualizations of the anatomic context of mycangia enabled by the integrated software.

Non-English Abstract (Chinese Abstract)

摘要

食菌小蠹 (Coleoptera: Curculionidae: Scolytinae and Platypodinae)是一类以取食其共生真菌的甲虫。食菌小蠹通过一种特殊结构——储菌囊，来保存和运送真菌。虽然储菌囊对于研究小蠹共生关系至关重要，但是由于其结构细微且脆弱，相关研究的进展十分困难。在此，我们通过使用最新的可视化扫描技术（显微CT扫描、LAT扫描）对比传统的石蜡切片，发现显微CT扫描在探索器官结构上具有潜力，而石蜡切片方法在展现细胞级别结构上依然有着无法取代的地位。实验室中，我们成功对比了多种食菌小蠹样本：*Ambrosiodmus minor* (Stebbing) 1909、*Euplatypus compositus* (Say) 1823、*Premnobius cavipennis* Eichhoff 1878、*Scolytoplatypus raja* Blandford 1893、*Xylosandrus crassiusculus* (Motschulsky) 1866和 *X. amputatus* (Blandford) 1894。发现三种类型的储菌囊（口器型、中胸型和前胸型）都可以在显微CT扫描下发现，我们还三维重建了*X. amputatus*的储菌囊与其周围的肌肉组织，显微CT扫描相比传统石蜡切片方法在探索内部结构上有着简单、可重建、可区分自然变形和软件数据化的优势。

Key words: laser ablation tomography (LATscan), paraffin sectioning, X-ray, muscle, Scolytinae

The field of insect anatomy has traditionally relied upon careful dissection, staining and sectioning of tissue samples. Although scanning electron microscopes (SEM) and transmission electron microscopes (TEM) have revolutionized our understanding of insect structure and function on a cellular level, samples require comparatively complicated preparation and are irrecoverable post visualization. Recently, new advances in the field of micro-computed tomography (micro-CT), laser ablation tomography (LATscan), and other methods have emerged, to potentially once again revolutionize the field.

New technologies are particularly important for the discovery of new morphological structures. While general insect anatomy has been well documented, there remain many poorly studied taxa and unusual or specialized organs. Included in the latter category are organs associated with symbioses, such as mycetomes, bacteriomes, or mycangia (Batra 1963, Francke-Grosmann 1963). The most interesting, but also the most challenging, feature of such organs is that they may have evolved many times independently, and therefore, their location and structure are not homologous across insect taxa (Johnson et al. 2018).

Here we tested new approaches for the discovery and characterization of mycangia, the organs used for the transport of symbiotic fungi in ambrosia beetles (Batra, 1963, Francke-Grosmann 1963, Paine et al. 1997). The ambrosia beetles belong to the weevil subfamilies Scolytinae and Platypodinae (Coleoptera: Curculionidae) and include about 4,800 wood-boring species (Kirkendall et al. 2015). Some of these beetles are important forestry pests because they are able to transport and transmit a variety of fungal symbionts between their host trees, and some of these can be pathogenic to plants (Harrington et al. 2008, Hulcr and Dunn 2011). For example, *Raffaelea lauricola* (Ophiostomataceae), which causes Laurel wilt, is transmitted by *Xyleborus glabratus* Eichhoff 1877 (Harrington et al. 2011). Additionally, members of the Ambrosial *Fusarium* clade, which cause *Fusarium* dieback, are disseminated by *Euwallacea* spp. (Eskalen et al. 2012). The study of the diversity of symbiotic fungi within mycangia has progressed rapidly with the advent of next generation high-throughput sequencing technologies (Harrington et al. 2010, Kostovcik et al. 2015). However, knowledge of the physical structure of many species remains scant (Francke-Grosmann 1956, 1967; Schedl 1962; Nakashima 1975; Hulcr and Stelinski 2017). The highly evolved structures of the mycangium are located in different parts of the body, in accordance with the phylogenetic relationship of the beetle species (Francke-Grosmann 1967, Hulcr et al. 2015). Mycangia are difficult to study owing to their small size and delicate structure which is easily damaged during dissection or preparation of cross sections. The visual identification and physical separation of the mycangium from a mass of animal tissue, viewed under a microscope, requires considerable experience and knowledge of beetle morphology and anatomy. Study of tissues surrounding the mycangia such as the musculature suffers from the same problems.

Methods used to analyze the location and structure of mycangia in beetles include hand-dissections, paraffin sections, SEM, and TEM (Stone et al. 2007, Yuceer et al. 2011, Li et al. 2015). These techniques are time-consuming and sample preparation is complicated by the fragility of the mycangial microstructure. Most traditional imaging methodologies also only provide two-dimensional data. Currently, nano-CT technology is an increasingly used technique in zoological imaging, producing rapid three-dimensional (3D) visualizations of high-resolution morphological and anatomical data (Holdsworth and Thornton 2002, Metscher 2009, Faulwetter et al. 2013). Micro-CT uses X-ray imaging and computer-based interpretation to produce a 3D rendition of a sample. It is often utilized to image dry samples of approximately 1~200 mm in length, although it is capable of obtaining a resolution down to approximately 0.1 µm, permitting the study of smaller structures (of less than 1 µm in length). Several studies have already shown the potential of micro-CT techniques to deliver novel data for investigating functional morphology in beetles (Li et al. 2011, van de Kamp et al. 2011, Wilhelm et al. 2011, Hörnschemeyer et al. 2013, Li et al. 2018). Paraffin sections have been utilized for about 150 yr (Van den Tweel and Taylor 2010), and with improved stains and tissue processors, this method remains in extensive use in biology and medicine to this day (Titford 2006). Sample preparation for paraffin sectioning involves infiltrating fixed and dehydrated tissues with molten paraffin wax, which hardens to provide support for sectioning. Following sectioning, sections are de-waxed, stained, and photographed using a camera mounted to a compound microscope (Celis et al. 2005). LATscan is a recently developed technique developed by the Roots lab at Pennsylvania State University (http://plantscience.psu.edu/research/labs/roots). LATscan uses a high-powered laser to repeatedly vaporize a thin surface layer of a specimen. Images of the specimen are simultaneously captured using a proprietary imaging system (patent US9976939B2). In this study, we compare the application of micro-CT with LATscan and paraffin sectioning in mycangial structure, and explore the potential of micro-CT to examine and reconstruct the physical structure of the mycangia in ambrosia beetles.

Materials and Methods

Specimen Preparation

Eight representative ambrosia beetle species, represented by at least two specimens each, were selected from the cryopreserved collection of the University of Florida Forest Entomology Collection (Table 1).

Table 1. Overview of scanned ambrosia beetle specimens

Mycangium	Species	Locality	Scan method and individuals (amt)
Oral	*Ambrosiophilus atratus* (Eichhoff) 1875	United States: NC: Alligator River United States: WV: Morgantown	Paraffin section (10), LAT(2)
Oral	*Ambrosiodmus minor* (Stebbing) 1909	United States: FL: Gainesville	Micro-CT(2), Paraffin section (11)
Oral	*Euwallacea interjectus* (Blandford) 1894	United States: FL: Gainesville	LAT(2)
Oral	*Premnobius cavipennis* Eichhoff 1878	United States: FK: Miami	Paraffin section (5), Micro-CT(1)
Mesonotal	*Xylosandrus amputatus* (Blandford) 1894	China: Guizhou: Guiyang	Micro-CT(3)
Mesonotal	*X. crassiusculus* (Motschulsky) 1866	United States: FL: Gainesville	Micro-CT(4)
Pronotal	*Euplatypus compositus* (Say) 1823	United States: FL: Gainesville	Micro-CT(3)
Pronotal	*Scolytoplatypus raja* Blandford 1893	China: Guizhou: Guiyang	Micro-CT(2)

All beetles had previously been collected using alcohol-baited traps that capture flying beetles. This was intentional because the mycangia of ambrosia beetles are most developed during the beetle's flight dispersal stage (Li et al. 2018). Specimens were preserved in 95% ethanol prior to treatment and identified with the aid of a stereomicroscope using the most recent taxonomic literature for the group (Beaver and Gebhardt 2006, Rabaglia et al. 2006, Gomez et al. 2018).

Micro-CT Imaging

Prior to scanning, specimens were dehydrated in a graded series of ethanol (from 95% to 100%) and dried at the critical point (Hitachi hcp-2, Hitachi Inc., Tokyo, Japan) or room temperature. All beetles were scanned with a MicroXCT-400 (Xradia Inc., California; beam strength: 60 kV, absorption contrast) at the Institute of Zoology, Chinese Academy of Sciences, China. *Xylosandrus crassiusculus* (Motschulsky) 1866 was also scanned with a Phoenix v|tomel|x M (GEs Measurement & Control business, Boston, MA) at the University of Florida's Nanoscale Research Facility, using a 180 kV X-ray tube with a diamond-tungsten target, at 90 kV, 400 mA, and with a one second detector time. Raw X-ray data were processed using GEs proprietary datos|x software v 2.3 to produce a series of tomogram images. The resulting sectioned images were of a resolution of approximately 1 µm.

Laser Ablation Tomography

Laser scans were undertaken by LATscan (www.l4is.com) by the L4iS staff. The laser utilized for the results in this paper was a Coherent (5100 Patrick Henry Drive, Santa Clara, CA 95054). Avia 355–7000 Q-switched ultraviolet laser source was used with a pulse repetition rate between 25 and 40 kHz at 355 nm. Images of the cross-section of the sample were captured via a Canon 70D equipped with a Canon Macro Photo Lens MP-E 65 mm 1:2.8 1-5X at 1 µm/pixel resolution.

Paraffin Section and Imaging

Paraffin sectioning was completed according to the procedure in Li et al. (2015). Heads were aseptically removed from the pronotum before sectioning. Once removed, beetle heads were fixed in 10% neutral buffered formalin (StatLab Medical Products) for 24 h and then soaked in phenol for 6 d at room temperature. Heads were treated with an automated tissue processor (Shandon Excelsior-Serial # EX01110212) to allow desiccation of tissues and infiltration of paraffin and subsequently embedded in paraffin blocks. We used a Microm HM 325 rotary microtome (Walldorf, Germany) to cut 10-µm transverse sections. Selected slides containing mycangia were confirmed by immediate observation, and were dried at 58°C in a lab oven (Boekel 107800) for 3 d, then stained with Harris-hematoxylin (Richard Allan Scientific # 7211) and eosin-phloxine (Surgipath # 080117), and examined and photographed using a Nikon Eclipse E600 compound microscope (Nikon Instruments, Melville, NY) with a Nikon Digital Sight DS-Ri1 high-resolution microscope camera to acquire brightfield images.

3D Reconstruction Model

The micro-CT image stacks obtained were imported into Amira 5.4.1 (Visage Imaging, San Diego, CA) and VG StudioMax 2.2 (Volume Graphics, Heidelberg, Germany) for 3D reconstructions, with which the 3D models were generated and drawn. Maya 2014 (Autodesk, Inc. San Rafael, CA) was used to smooth and render the 3D models. The final figures were edited and prepared using Photoshop and Illustrator (Adobe, San Jose, CA).

Results

Comparison of Micro-CT, LATscan, and Paraffin Sectioning to Visualize Mycangia

The oral mycangia of four ambrosia beetles: *Ambrosiophilus atratus* (Eichhoff) 1875, *Ambrosiodmus minor* (Stebbing) 1909, *Euwallacea interjectus* (Blandford) 1894 and *Premnobius cavipennis* Eichhoff 1878 were visualized by Micro-CT, LATscan, or paraffin sectioning (Table 1, Figs. 1 and 2). The mycangia (Fig. 1, white/black arrows) and the fungal mass (Fig. 2, red arrows) were all visible through all three methods. The mycangial lumen appears largely exposed to the oral cavity. Mycangia were easily located within the scanned sections. The three methods yielded distinctive results, each with specific benefits and disadvantages. These benefits and disadvantages are summarized in Table 2. Considering their respective properties, micro-CT is the best option for rapid and nondestructive imaging, although having the drawback of being achromatic.

Comparison of Mycangial Structures Visualized With Micro-CT

Although the entire body of each beetle specimen was scanned, only the portion containing the mycangium is presented here (Fig. 3A–G). Micro-CT scanning resulted in high-contrast and high-definition visualizations of all selected mycangial structures. The mycangia (Fig. 3, white arrows) and the fungal mass (Fig. 3, yellow arrows) were distinguishable from each other. The mesonotal mycangium in *Xylosandrus* has a single entry but diverges into a pair of separate semi-spiral pouches (Fig. 3C). It is composed of pouches formed by the intersegmental membrane between the pronotum and the scutellum. Changing the imaging plane allowed for partly filled mycangia to be observed (Fig. 3A and B). The micro-CT sections (Fig. 3D and E) indicated that *Scolytoplatypus* has a single pronotal mycangium, under the pronotal surface, that is covered by a membrane, forming a pocket. Many muscles surround the mycangium. The scans reveal the mycangia of *E. compositus* to be composed of shallow cavities in the chitinous exoskeleton of the dorsal surface of the pronotum (Fig. 3F and G). No membranous tissue was detected in the pronotal pits. The fungal load can be asymmetrical—one of the mycangial pocket in our specimens was empty and the other one full. Glands and secretory cells were invisible in the micro-CT scan of all samples.

3D Reconstruction of a Mesonotal Mycangium

A 3D reconstruction of the mycangium (and associated muscles) in *Xylosandrus amputatus* (Blandford) 1894 is shown in Fig. 4. The following terminology is used for the structure of the musculature associated with the mycangium, which is mainly adapted from Ge et al. (2007) and Friedrich and Beutel (2008). Prothorax musculature (Fig. 4D): *M.1* M. scutello-occipitalis 1°, slender, with four bundles; origin of M.1: ventral-median scutellum; insertion of M.1: dorsolateral postocciput; function: movement of head capsule. *M.2* M. scutello-occipitalis 2°, slender, with two bundles; origin of M.2: lateral scutellum, insertion of M.2: dorsolateral postocciput, function: movements of the head capsule. *M.3* M. scutello-pronotalis 1°, well developed, with two major bundles and two minor bundles; origin of M.3: median pronotum; insertion of M.3: dorsolateral postocciput; function: movement of pronotum. *M.4* M. pronoto-occipitalis 2°, well developed, with two bundles cross with each other, each bundle consists of four sub-bundles, the eight sub-bundles alternately cross with each other (resembles crossed fingers); origin of M.4: posteromedian pronotum; insertion of M.4: dorsolateral postocciput; function: movements of the head, each major bundle is responsible for either the rightwards or

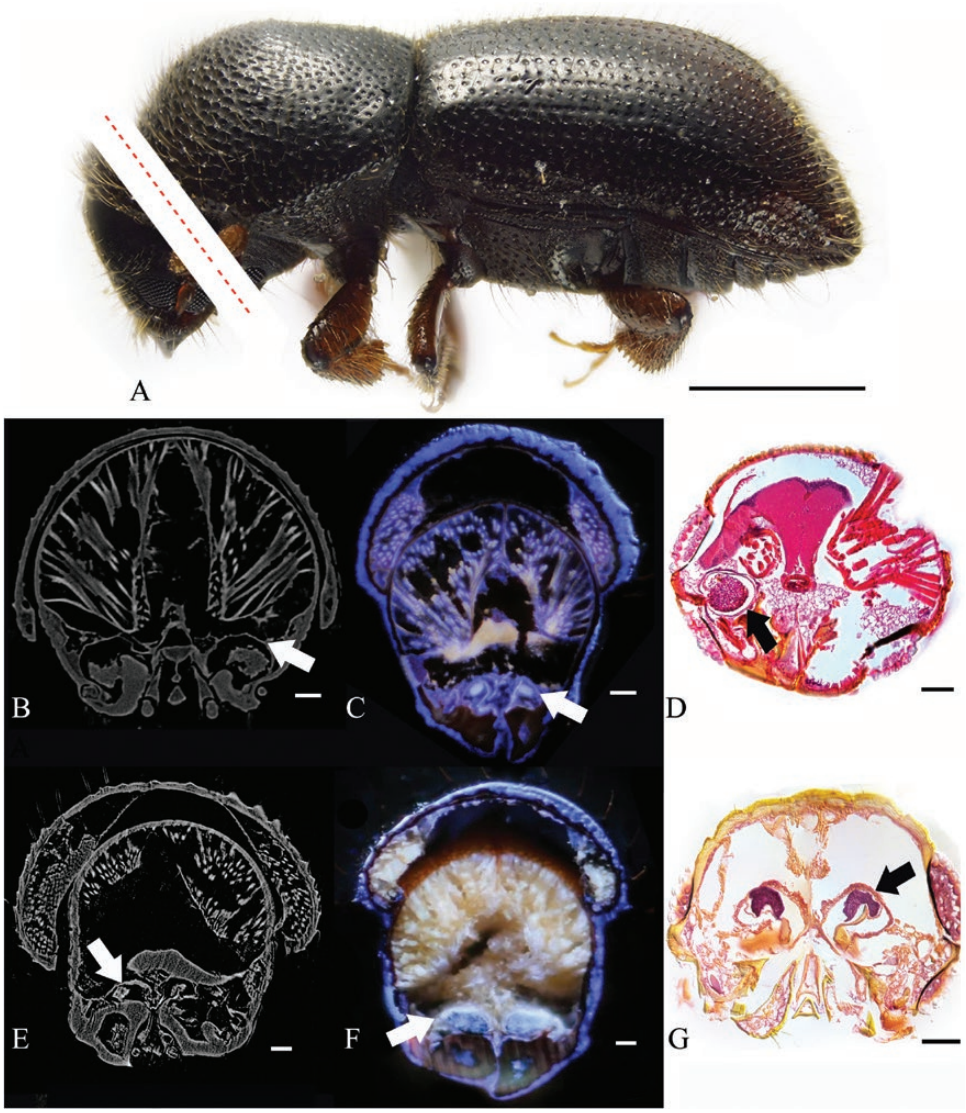

Fig. 1. Cross-sections of oral mycangia from ambrosia beetle; (A)(C) *Ambrosiophiuls atratus*; red dotted line digitally illustrating the location of sections only, not actual photographs; (B)(D) *Premnobius cavipennis*; (E)(G) *Ambrosiodmus minor*; (F) *Euwallacea interjectus*; (B)(E) micro-CT; (C)(F) LATscan; (D)(G) paraffin section; white/black arrows: mycangial membrane; scales bar, (A) 1 mm; (B–J) 0.1 mm.

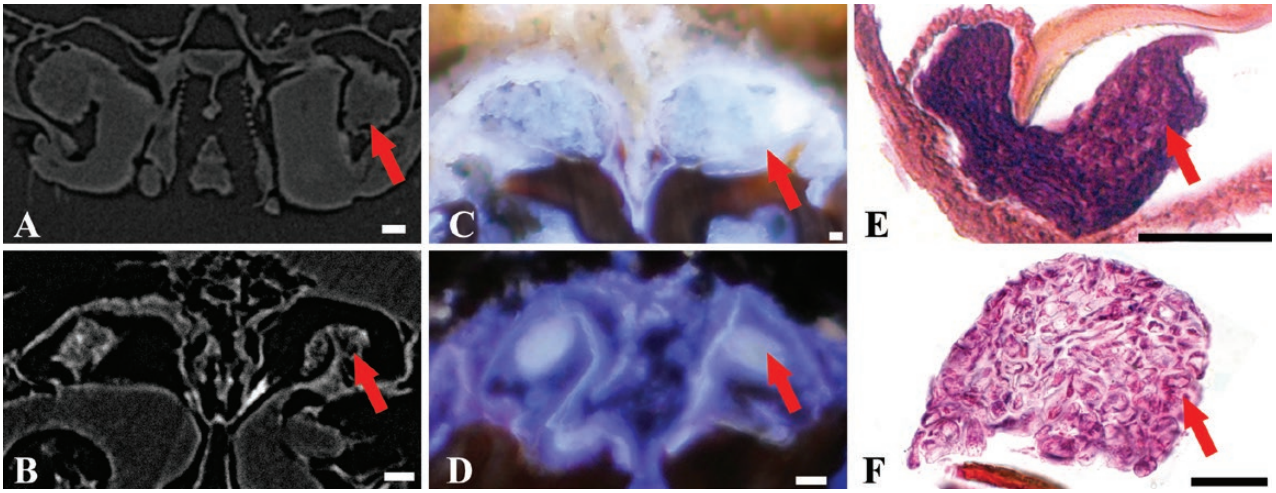

Fig. 2. Cross-sections of fungal inoculum in oral mycangia from ambrosia beetles; (A) *Premnobius cavipennis*; (B)(E) *Ambrosiodmus minor*; (C) *Euwallacea interjectus*; (D)(F) *Ambrosiophilus atratus*; red arrows: fungal inoculum; (A)(B) micro-CT; (C)(D) LATscan; (E)(F) paraffin section; scales bar, 25 μm.

Table 2. Comparison of the features of Micro-CT, LAT, and Paraffin sectioning used in the visualization of the internal structure of bark and ambrosia beetles

Methods	Time to sample beetle	Sample preparation	Resolution	Invasive to specimens	Price ($)	References
LAT (LATscan)	2–5 h	Dry	Depend on microscope and camera	Yes	1,100 (in 2016)	http://plantscience.psu.edu/research/labs/roots/sites/laserfacility
Micro-CT	1–3 h	Dry	0.5–5 µm	No	100–200	Friedrich et al. 2014, Ruan et al. 2016
Paraffin section with brightfield microscopy	>24 h	Paraffin seal	Depend on microscope and camera, but >3 µm	Yes	50–200	Bancroft and Gamble 2008, Gijtenbeek et al. 2006, Lowe and Anderson 2014

Time and price are estimated for one beetle specimen.

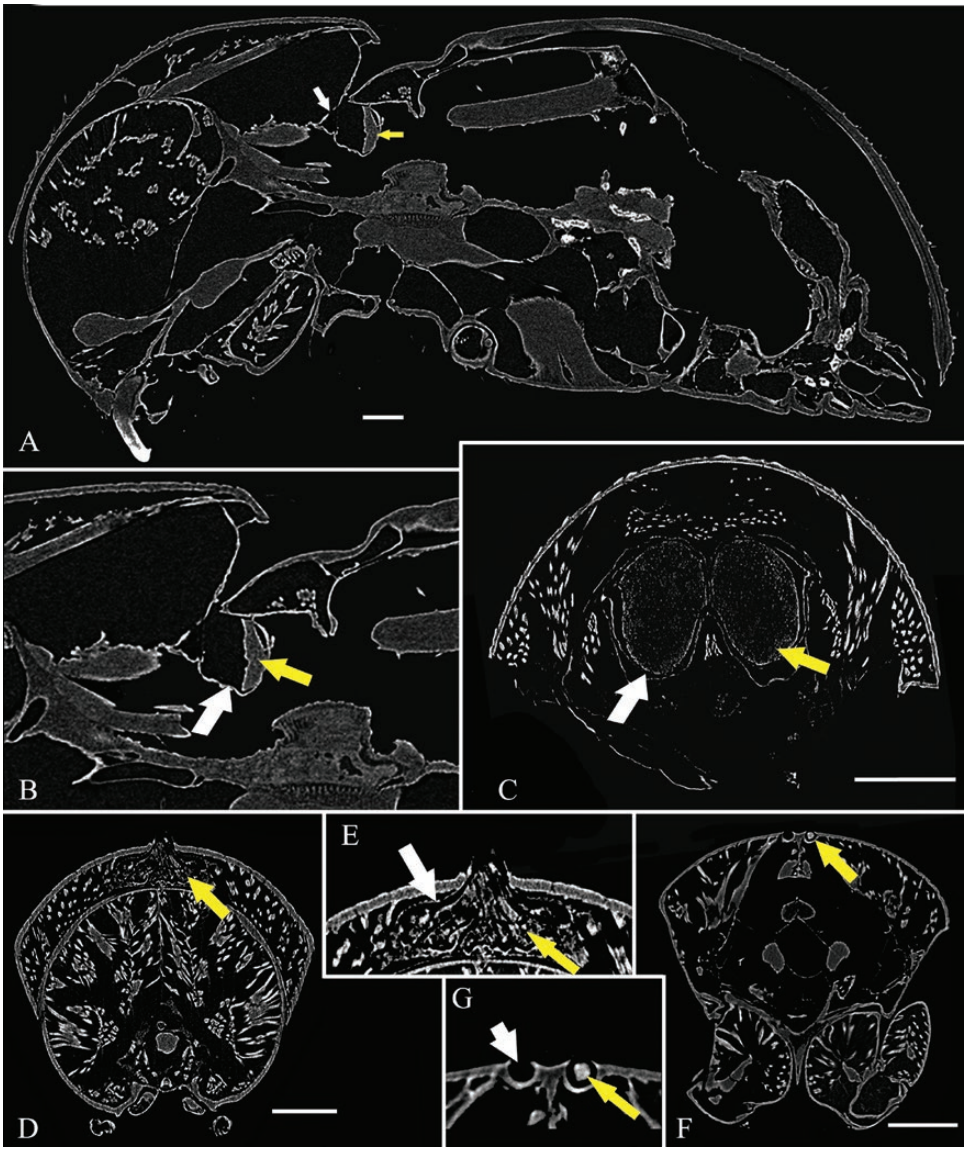

Fig. 3. Micro-CT micrographs of ambrosia beetles in lateral section (A–B) and cross section (C–G), and (A) *Xylosandrus crassiusculus*, mesonotal mycangium; (B) magnification of mycangium in *X. crassiusculus*; (C) *X. amputatus*, mesonotal mycangium; (D) *Scolytoplatypus raja*; pronotal mycangium; (E) magnification of mycangium in *S. raja*; (F) *Euplatypus compositus*; pronotal mycangium; (G) magnification of mycangium in *E. compositus*; white arrows: mycangial membrane; yellow arrows: fungal inoculum. Scales bar, 0.25 mm.

leftwards movement of the head, minor bundles are responsible for more precise movements. *M.5* M. pronoto-coxalis, well developed; origin of M.5: posterior pronotum; insertion of M.5: pro-coxa; function: movements of the pro-coxa. M.1 and M.2 bypass the mycangium and attach to the scutellum. The posterior of M.3 is close to mycangia.

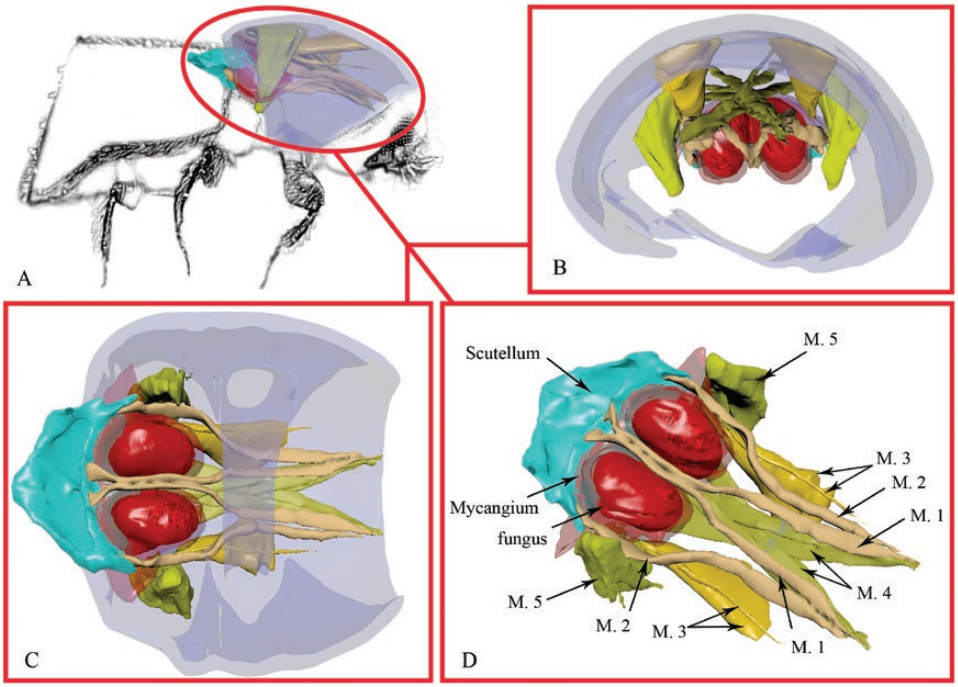

Fig. 4. 3-D reconstruction of prothorax and mesonotum for *X. amputatus* based on micro-CT scans; A: lateral side; B: frontal view; C: ventral view; D: mycangium with prothorax musculature nearby. M.1: M. scutello-occipitalis 1°; M.2: M. scutello-occipitalis 2°; M.3: M. scutello-pronotalis; M.4: M. pronoto-occipitalis; M.5: M. pronoto-coxalis.

Discussion

Both the paraffin sectioning technique and LATscan are useful methods to provide images of the internal structures with tissues resolved into different colors (Gebhardt et al. 2004, Kasson et al. 2013, Li et al. 2015). Paraffin sectioning is time-consuming and requires experience and skill. Furthermore, controlling the angle of sectioning is also difficult, and asymmetric sections are common (Fig. 1D). Nevertheless, sectioning has been very important in studying beetle structures, and still remains the only method that permits a high enough resolution to show fungal cells within mycangia (Fig. 2; Kasson et al. 2013, Li et al. 2015, Kasson et al. 2016, Bateman et al. 2017). LATscan and micro-CT are able to recover high-resolution 3D structures. Currently, LATscan appears more expensive for the end user, but our conclusion does not take into consideration the price of the nano-CT equipment and the economy of scale in the future. Even though micro-CT cannot reproduce color graphics that enable the different tissues to be distinguished, its high resolution enables the membranal mycangium of ambrosia beetle to be successfully visualized. Micro-CT is the most rapid of the three techniques.

In the present study, four different types of mycangia were successfully re-confirmed and distinguished in situ using non-invasive micro-CT scanning (Figs. 1 and 3). The mycangia of *Ambrosiodmus*, *Xylosandrus*, and *Scolytoplatypus* are distinctly formed of an outer membrane, within which the symbiotic fungus is contained. These cross sections of scolytid beetles reveal the same structures observed by Francke-Grosmann (1956, 1967) and Schedl (1962), except for the massive mycangia under the mesonotum (Fig. 3C). Various authors suggest that the outer membranes of mycangia contain glands producing important secretions (Francke-Grosmann 1956, 1967; Barras and Perry 1971; Paine and Birch 1983; Six 2003; Stone et al. 2007). Six (2003) described the membranous mycangium structure as glandular and, in reference to *Euplatypus*, the hard, concave exoskeletal structure, as the non-glandular mycangium. Even though shape of mycangia were distinct in micro-CT scans, neither glands nor secretory cells were visible. Which may be attributed to two reasons: 1) although theoretically micro-CT can achieve a peak resolution of 0.5 µm, the finest resolution we obtained was between 0.5 and 1.0 µm owing to the small size (only about 2 mm long) and hard cuticle of the beetles. This resolution is insufficient to visualize fine structures that may be only a few cells thick; and 2) prior to the study, our samples had been cryopreserved in ethanol and dried at the critical point or room temperature first. The freeze and dehydration may have resulted in some of the morphological features of the mycangia and fungal propagule being difficult to observe.

The relationship between the mycangium and its associated musculature has not been previously studied on account of the limited technology previously available permitting such investigations (Schedl 1962, Francke-Grosmann 1967). The 3D reconstructed models presented here revealed more detail than hand dissections. Because the nomenclature for musculature used in some previous works is now out of date (Francke-Grosmann 1956, 1967; Schedl 1962), a new nomenclature, which has recently been widely adopted was used here (Beutel and Haas 2000, Ge et al. 2007. Friedrich and Beutel 2008). Our visualizations of the mycangia of *X. crassiusculus* and *X. amputatus* agree with the illustrations of those of *X. compactus* and *X. discolor* by Schedl (1962), which show that mesonotal mycangia lie between the pronotum and the scutellum. However, our visualization of the associated musculature showed differences. For instance, muscle M.4 (M. pronoto-occipitalis) in *X. compactus* and *X. discolor*, as illustrated by Schedl (1962), has a single bundle, yet our 3D reconstructed model (Fig. 4) reveals that M.4 in *X. amputatus* is comprised of two muscular bundles which both split to four sub-bundles as they cross, with each sub-bundle alternately crossing each other as they connect from the right side of the scutellum to the left side of the head (and vice versa). With this level of detail, the function of M.4 can be more specifically and precisely inferred. Furthermore, we have seen that four bundles of M.3 are connected to the posterior of the pronotum. The anterior end of the muscle

fascicles are inserted into the dorsolateral pronotum. The movement of the scutellum by M.1 and M.2 may have similar effects. It is plausible that longitudinal contraction of M.1, M.2, and M.3 will tightly constrict the mycangium. Muscle M.5 and M.3 appear much stronger than as described by Schedl (1962). Francke-Grosmann (1956) and Schedl (1962) believed the contraction of these muscles would cause the deformation of the mycangium as the beetle bores a gallery. Whether this mechanism plays a part in absorbing and releasing fungal propagule in this functional context is not clear. Unfortunately, as with the mycangia, the muscle tissues may also have been damaged during storage and dehydration. Future observations should be conducted with individuals placed in fixative alive or freshly dead.

Besides micro-CT, and related X-ray tomography, many alternative methods with a 3D imaging capability exist, such as confocal laser scanning microscopy (CLSM), magnetic resonance imaging (MRI), focused ion beam SEM (FIB-SEM), as well as LATscan mentioned here. Compared to these techniques, micro-CT and related X-ray tomography offer many advantages for the visualization of mycangia. These include the non-invasive nature of micro-CT, its high resolution, and its ability to produce high-resolution 3D images with isotropic spatial resolution in all three dimensions. Since the mycangia of ambrosia beetles are fragile, usually consisting of only a thin membrane, these advantages make this technique highly useful in the research on the beetle-fungus symbiosis. The fast scanning speed of generally less than 1 h (e.g., 10~30 min, depending on the desired resolution and the samples, is also advantageous (Friedrich et al. 2014, Walton et al. 2015, Ruan et al. 2016). Despite this, conventional optical light microscopy currently remains the most common imaging system employed by researchers due to its affordability, simplicity, and because it permits the study of live individuals. Future improvements in the image resolution and the user-friendliness of Micro-CT techniques should lead to their greater use in biological research.

A variety of other insects possess mycangia, including wood wasps (Morgan 1968), leaf-rolling weevils (Li et al. 2012), phoretic mites (Mori et al. 2011), and gall midges (Borkent and Bissett 1985), and all such mycangia serve as fungal repositories. The techniques tested here may be equally effective in the exploration of these mycangia.

Acknowledgments

We thank the four anonymous reviewers who help improving the manuscript and to Asheesh Lanba (L4iS) for comments on the LATscan methods section. Y.L., A.J.J., C.P.D.T.G., and J.H. were funded by the United States Department of Agriculture (USDA) Forest Service, USDA APHIS Farm Bill section 10007, Florida Department of Agriculture and Consumer Services – Division of Plant Industry, and the National Science Foundation (DEB 1556283).

References Cited

Bancroft, J. D., and M. Gamble. 2008. Theory and practice of histological techniques. London, UK Elsevier Health Sciences.

Barras, S. J., and T. Perry. 1971. Gland cells and fungi associated with prothoracic mycangium of *Dendroctonus adjunctus* (Coleoptera: Scolytidae). Ann. Entomol. Soc. Am. 64: 123–126.

Bateman, C., Y-T. Huang, D. R. Simmons, M. T. Kasson, E. L. Stanley, and J. Hulcr. 2017. Ambrosia beetle *Premnobius cavipennis* (Scolytinae: Ipini) carries highly divergent ascomycotan ambrosia fungus, *Afroraffaelea ambrosiae* gen. nov. et sp. nov. (Ophiostomatales). Fungal Ecol. 25: 41–49.

Batra, L. R. 1963. Ecology of ambrosia fungi and their dissemination by beetles. Trans. Kans. Acad. Sci. 66: 213–236.

Beaver, R. A., and H. Gebhardt. 2006. A review of the Oriental species of *Scolytoplatypus* Schaufuss (Coleoptera, Curculionidae, Scolytinae). Deut. Entomol. Z. 53: 155–178.

Beutel, R. G., and F. Haas. 2000. Phylogenetic relationships of the suborders of Coleoptera (Insecta). Cladistics. 16: 103–141.

Borkent, A., and J. Bissett. 1985. Gall midges (Diptera: Cecidomyiidae) are vectors for their fungal symbionts. Symbiosis. 1: 185–194.

Celis, J. E., N. Carter, K. Simons, J. V. Small, T. Hunter, and D. Shotton. 2005. Cell biology, four-volume set: a laboratory handbook. Academic Press San Diego, California.

Eskalen, A., A. Gonzalez, D. Wang, M. Twizeyimana, J. Mayorquin, and S. Lynch. 2012. First report of a *Fusarium* sp. and its vector tea shot hole borer (*Euwallacea fornicatus*) causing *Fusarium* dieback on avocado in California. Plant Dis. 96: 1070–1070.

Faulwetter, S., A. Vasileiadou, M. Kouratoras, D. Thanos, and C. Arvanitidis. 2013. Micro-computed tomography: introducing new dimensions to taxonomy. ZooKeys. 263: 1–45.

Francke-Grosmann, H. 1956. Hautdrüsen als träger der pilzsymbiose bei ambrosiakäfern. Z. Morphol. Oekol Tiere. 45: 275–308.

Francke-Grosmann, H. 1963. Some new aspects in forest entomology. Annu. Rev. Entomol. 8: 415–438.

Francke-Grosmann, H. 1967. Ectosymbiosis in wood-inhabiting insects, pp. 141–205. *In* H. SM (ed.), Symbiosis: Associations of invertebrates, birds, ruminants, and other biota, vol. 2. Academic Press, New York, NY.

Friedrich, F., and R. G. Beutel. 2008. The thorax of *Zorotypus* (Hexapoda, Zoraptera) and a new nomenclature for the musculature of Neoptera. Arthropod Struct. Dev. 37: 29–54.

Friedrich, F., Y. Matsumura, H. Pohl, M. Bai, T. Hoernschemeyer, and R. G. Beutel. 2014. Insect morphology in the age of phylogenomics: innovative techniques and its future role in systematics. Entomol. Sci. 17: 1–24.

Ge, S., R. G. Beutel, and X. Yang. 2007. Thoracic morphology of adults of Derodontidae and Nosodendridae and its phylogenetic implications (Coleoptera). Syst. Entomol. 32: 635–667.

Gebhardt, H., D. Begerow, and F. Oberwinkler. 2004. Identification of the ambrosia fungus of *Xyleborus monographus* and *X. dryographus* (Coleoptera: Curculionidae, Scolytinae). Mycol. Prog. 3: 95–102.

Gijtenbeek, J. M., P. Wesseling, C. Maass, L. Burgers, and J. A. van der Laak. 2006. Three-dimensional reconstruction of tumor microvasculature: simultaneous visualization of multiple components in paraffin-embedded tissue. Angiogenesis. 8: 297.

Gomez, D. F., R. J. Rabaglia, K. E. O. Fairbanks, J. Hulcr. 2018. North American Xyleborini north of Mexico: a review and key to genera and species (Coleoptera, Curculionidae, Scolytinae). ZooKeys. 768: 19–68.

Harrington, T. C., S. W. Fraedrich, and D. N. Aghayeva. 2008. *Raffaelea lauricola*, a new ambrosia beetle symbiont and pathogen on the Lauraceae. Mycotaxon. 104: 399–404.

Harrington, T. C., D. N. Aghayeva, and S. W. Fraedrich. 2010. New combinations in *Raffaelea*, *Ambrosiella*, and *Hyalorhinocladiella*, and four new species from the redbay ambrosia beetle, *Xyleborus glabratus*. Mycotaxon. 111: 337–361.

Harrington, T. C., H. Y. Yun, S. S. Lu, H. Goto, D. N. Aghayeva, and S. W. Fraedrich. 2011. Isolations from the redbay ambrosia beetle, *Xyleborus glabratus*, confirm that the laurel wilt pathogen, *Raffaelea lauricola*, originated in Asia. Mycologia. 103: 1028–1036.

Holdsworth, D. W., and M. M. Thornton. 2002. Micro-CT in small animal and specimen imaging. Trends Biotechnol. 20: S34–S39.

Hörnschemeyer, T., J. Bond, and P. G. Young. 2013. Analysis of the functional morphology of mouthparts of the beetle *Priacma serrata*, and a discussion of possible food sources. J. Insect Sci. 13: 126.

Hulcr, J., and R. R. Dunn. 2011. The sudden emergence of pathogenicity in insect-fungus symbioses threatens naive forest ecosystems. Proc. Biol. Sci. 278: 2866–2873.

Hulcr, J., and L. L. Stelinski. 2017. The ambrosia symbiosis: from evolutionary ecology to practical management. Annu. Rev. Entomol. 62: 285–303.

Hulcr, J., T. H. Atkinson, A. I. Cognato, B. H. Jordal, and D. D. McKenna. 2015. Morphology, taxonomy, and phylogenetics of bark beetles, pp. 41–84. *In* F. E. Vega and R. W. Hofstetter (eds.), Bark beetles: biology

and ecology of native and invasive species. Academic Press, San Diego, California.

Johnson, A. J., D. D. McKenna, B. H. Jordal, A. I. Cognato, S. M. Smith, A. R. Lemmon, E. M. Lemmon, and J. Hulcr. 2018. Phylogenomics clarifies repeated evolutionary origins of inbreeding and fungus farming in bark beetles (Curculionidae, Scolytinae). Mol. Phylogenet. Evol. 127: 229–238.

Kasson, M. T., K. O'Donnell, A. P. Rooney, S. Sink, R. C. Ploetz, J. N. Ploetz, J. L. Konkol, D. Carrillo, S. Freeman, Z. Mendel, et al. 2013. An inordinate fondness for Fusarium: phylogenetic diversity of fusaria cultivated by ambrosia beetles in the genus Euwallacea on avocado and other plant hosts. Fungal Genet. Biol. 56: 147–157.

Kasson, M. T., K. L. Wickert, C. M. Stauder, A. M. Macias, M. C. Berger, D. R. Simmons, D. P. Short, D. B. DeVallance, and J. Hulcr. 2016. Mutualism with aggressive wood-degrading *Flavodon ambrosius* (Polyporales) facilitates niche expansion and communal social structure in *Ambrosiophilus* ambrosia beetles. Fungal Ecol. 23: 86–96.

Kirkendall, L. R., P. H. Biedermann, and B. H. Jordal. 2015. Evolution and diversity of bark and ambrosia beetles, pp. 85–156. *In* F. E. Vega and R. W. Hofstetter (eds.), Bark beetles: biology and ecology of native and invasive species. Academic Press, San Diego, California.

Kostovcik, M., C. C. Bateman, M. Kolarik, L. L. Stelinski, B. H. Jordal, and J. Hulcr. 2015. The ambrosia symbiosis is specific in some species and promiscuous in others: evidence from community pyrosequencing. ISME J. 9: 126–138.

Li, D., K. Zhang, P. Zhu, Z. Wu, and H. Zhou. 2011. 3D configuration of mandibles and controlling muscles in rove beetles based on micro-CT technique. Anal. Bioanal. Chem. 401: 817–825.

Li, X., W. Guo, and J. Ding. 2012. Mycangial fungus benefits the development of a leaf-rolling weevil, *Euops chinesis*. J. Insect Physiol. 58: 867–873.

Li, Y., L. You, D. R. Simmons, C. C. Bateman, D. P. Short, M. T. Kasson, R. J. Rabaglia, and J. Hulcr. 2015. New fungus-insect symbiosis: culturing, molecular, and histological methods determine saprophytic polyporales mutualists of *ambrosiodmus* ambrosia beetles. PLoS One 10: e0137689.

Li, Y., Y. Y. Ruan, E. L. Stanley, J. Skelton, and J. Hulcr. 2018. Plasticity of mycangia in *Xylosandrus* ambrosia beetles. Insect Sci. doi:10.1111/1744-7917.12590

Lowe, J. S., and P. G. Anderson. 2014. Stevens & lowe's human histology e-book: Online Access. Elsevier Health Sciences. Philadelphia, Pennsylvania

Metscher, B. D. 2009. MicroCT for developmental biology: a versatile tool for high-contrast 3D imaging at histological resolutions. Dev. Dyn 238: 632–640.

Morgan, F. D. 1968. Bionomics of Siricidae. Annu. Rev. Entomol. 13: 239–256.

Mori, B. A., H. C. Proctor, D. E. Walter, and M. L. Evenden. 2011. Phoretic mite associates of mountain pine beetle at the leading edge of an infestation in northwestern Alberta, Canada. Can. Entomol. 143: 44–55.

Nakashima, T. 1975. Several types of the mycetangia found in platypodid ambrosia beetles (Coleoptera: Platypodidae). Insecta Matsumurana. 7: 1–69.

Paine, T., and M. Birch. 1983. Acquisition and maintenance of mycangial fungi by *Dendroctonus brevicomis* LeConte (Coleoptera: Scolytidae). Environ. Entomol. 12: 1384–1386.

Paine, T. D., K. F. Raffa, and T. C. Harrington. 1997. Interactions among Scolytid bark beetles, their associated fungi, and live host conifers. Annu. Rev. Entomol. 42: 179–206.

Rabaglia, R. J., S. A. Dole, and A. I. Cognato. 2006. Review of American Xyleborina (Coleoptera: Curculionidae: Scolytinae) occurring north of Mexico, with an illustrated key. Ann. Entomol. Soc. Am. 99: 1034–1056.

Ruan, Y., D. Dan, M. Zhang, M. Bai, M. Lei, B. Yao, and X. Yang. 2016. Visualization of the 3D structures of small organisms via LED-SIM. Front. Zool. 13: 1–10.

Schedl, W. 1962. Ein Beitrag zur Kenntnis der Pilzübertragungsweise bei xylomycetophagen Scolytiden (Coleoptera). Osterreichische Akademie der Wissenschaften, Mathematisch-Naturwissenschtliche Klasse. 171: 363–387.

Six, D. L. 2003. Bark beetle-fungus symbioses, pp. 97–114. *In* K. Bourtzis and T. A. Miller (eds.), Insect symbiosis, vol. 1. CRC Press, Washington, DC.

Stone, W. D., T. E. Nebeker, W. A. Monroe, and J. A. MacGown. 2007. Ultrastructure of the mesonotal mycangium of *Xylosandrus mutilatus* (Coleoptera: Curculionidae). Can. J. Zool. 85: 232–238.

Titford, M. 2006. A short history of histopathology technique. J. Histotechnol. 29: 99–110.

Van de Kamp, T., P. Vagovič, T. Baumbach, and A. Riedel. 2011. A biological screw in a beetle's leg. Science. 333: 52.

Van den Tweel, J. G., and C. R. Taylor. 2010. A brief history of pathology. Virchows Arch. 457: 3–10.

Walton, L. A., R. S. Bradley, P. J. Withers, V. L. Newton, R. E. Watson, C. Austin, and M. J. Sherratt. 2015. Morphological characterisation of unstained and intact tissue micro-architecture by X-ray computed micro- and nano-tomography. Sci. Rep. 5: 1–14.

Wilhelm, G., S. Handschuh, J. Plant, and H. L. Nemeschkal. 2011. Sexual dimorphism in head structures of the weevil *Rhopalapion longirostre* (Olivier 1807)(Coleoptera: Curculionoidea): a response to ecological demands of egg deposition. Biol. J. Linn. Soc. 104: 642–660.

Yuceer, C., C. Y. Hsu, N. Erbilgin, and K. D. Klepzig. 2011. Ultrastructure of the mycangium of the southern pine beetle, *Dendroctonus frontalis* (Coleoptera: Curculionidae, Scolytinae): complex morphology for complex interactions. Acta Zool. 92: 216–224.